Le point-sur/Review article

Elastic properties of glasses: a multiscale approach

Tanguy Rouxel

Mécanique des Matériaux Fragiles, LARMAUR, FRE-CNRS 2717, bâtiment 10B, campus de Beaulieu, Université de Rennes 1, 35042 Rennes cedex, France

Available online 13 October 2006

Article written at the invitation of the Editors

Abstract

Very different materials are named 'Glass', with Young's modulus E and Poisson's ratio ν extending from 5 to 180 GPa and from 0.1 to 0.4, respectively, in the case of bulk inorganic glasses. Glasses have in common the lack of long range order in the atomic organization. Beside the essential role of elastic properties for materials selection in mechanical design, we show in this analysis that macroscopical elastic characteristics (E, ν) provide an interesting way to get insight into the short- and medium-range orders existing in glasses. In particular, ν, the packing density (C_g) and the glass network dimensionality appear to be strongly correlated. Networks consisting primarily of chains and layers units (chalcogenides, low Si-content silicate glasses) correspond to $\nu > 0.25$ and $C_g > 0.56$, with maximum values observed for metallic glasses ($\nu \sim 0.4$ and $C_g > 0.7$). On the contrary, $\nu < 0.25$ is associated to a highly cross-linked network with a tri-dimensional organization resulting in a low packing density. Moreover, the temperature dependence of the elastic moduli brings a new light on the 'fragility' of glasses (as introduced by Angell) and on the level of cooperativity of atomic movements at the source of the deformation process. ***To cite this article: T. Rouxel, C. R. Mecanique 334 (2006).***
© 2006 Académie des sciences. Published by Elsevier Masson SAS. All rights reserved.

Résumé

Propriétés élastiques des verres : approche multiéchelle. Sous l'appellation « verre » sont rassemblés des matériaux très différents qui ont en commun une organisation atomique dépourvue d'ordre à longue distance, avec un module de Young (E) et un coefficient de Poisson (ν) variant respectivement de 5 à 180 GPa et de 0,1 à 0,4 pour les verres inorganiques. A côté du rôle essentiel que jouent les propriétés élastiques pour le choix d'un matériau de construction et le calcul de structure, nous montrons dans cette revue que les caractéristiques élastiques macroscopiques (E, ν) permettent de sonder l'ordre à courte et à moyenne distance existant dans la plupart des verres. En particulier, une excellente corrélation existe entre ν, la densité d'empilement (C_g) et la dimensionnalité du réseau vitreux. Pour $\nu > 0,25$, on a $C_g > 0,56$, ce qui indique que le verre est principalement constitué de chaînes et de feuillets (chalcogénures, verres silicatés riches en cations compensateurs et modificateurs de réseau). Les maxima de ν et C_g sont atteints pour les verres métalliques ($\nu \sim 0,4$ et $C_g > 0,7$). Au contraire, lorsque $\nu < 0,25$, cela correspond à une grande réticulation et une organisation tri-dimensionnelle s'accompagnant d'une faible compacité. En outre, la dépendance des modules d'élasticité avec la température apporte un éclairage original sur la « fragilité » (au sens de Angell) des verres et sur le degré de coopérativité des mouvements des atomes à l'origine de la déformation. ***Pour citer cet article : T. Rouxel, C. R. Mecanique 334 (2006).***
© 2006 Académie des sciences. Published by Elsevier Masson SAS. All rights reserved.

Keywords: Continuum mechanics; Glass; Multiscale approach; Elastic moduli

Mots-clés : Milieux continus ; Verre ; Approche multiéchelle ; Modules d'élasticité

E-mail address: tanguy.rouxel@univ-rennes1.fr (T. Rouxel).

1. Introduction

1.1. The different glass systems

Even although the search for glasses possessing high elastic moduli is a relatively old topic, it is of paramount interest today with the need for new light and durable materials stiffer than those presently available. For instance, in order to increase both the rotating speed and the durability of computer hard disks, Al–Mg alloys are being more and more replaced by high Young's modulus (E) glasses. An enhancement of the elastic moduli allows also for a decrease of the weight of windows (for a given glass density) and thus for a significant decrease of the energy consumption in the transportation industry.

Elastic moduli give a global and often macroscopic view of a material stiffness. They reflect both the interatomic bonding energies and the connectivity. Therefore, they depend much on the glass composition. For instance, pure amorphous selenium [1], a glass from the YSiAlON system [2] and a $W_{46}Ru_{37}B_{17}$ metallic glass [3] will have Young's moduli of 10, 165 and 365 GPa respectively.

This review is focussed on inorganic glasses with extreme properties: high performance bulk metallic [3–8], rare earth [9–12], silico-aluminate [13–23], oxynitride [2,24–34] and oxycarbide [35–39] glasses on one side, and soft and fragile chalco-halogenide [40–45] glasses on the other side. Young's modulus (the most frequently measured elastic modulus) is plotted as a function of the glass transition temperature (T_g) in Fig. 1. Although the general tendency is an increase of E with T_g, it is noteworthy that the highest values for E are not reported for the most refractory glasses (SiOC glasses). This is because SiOC glasses, such as a-SiO_2, are characterized by a low atomic packing density, as will be further discussed. On the contrary, the high packing density of metallic glasses counterbalances their low bonding energy.

Even although ice is a mineral, there exist also different amorphous phases for solid water. The transition temperature T_g of amorphous ice is close to 136 K and E ranges between 8, for the low density phase ($\rho = 0.93$ g/cm^3), and
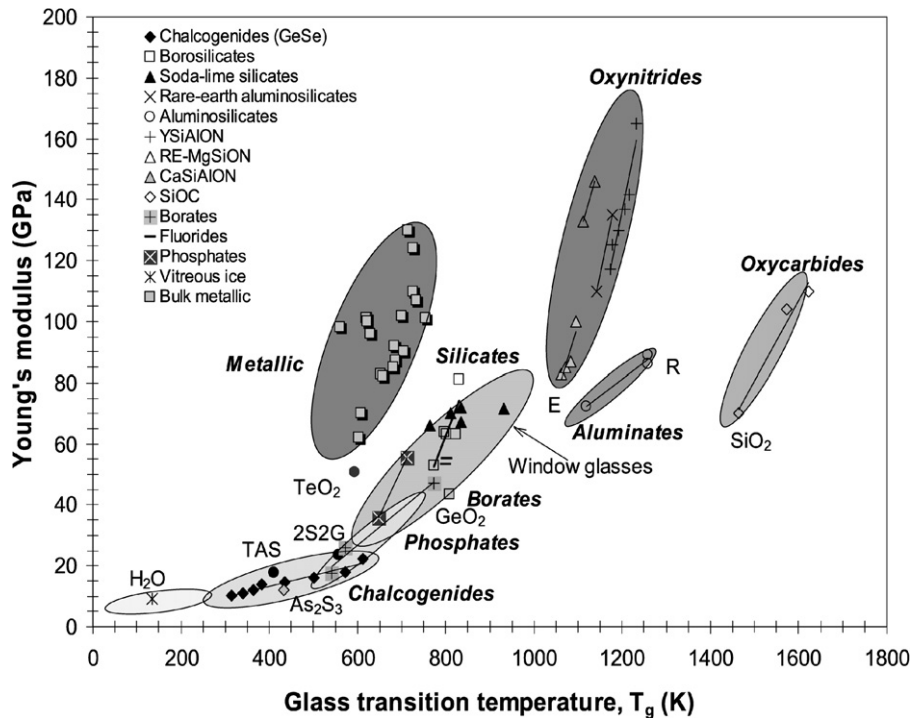

Fig. 1. Young's modulus at 293 K (except for amorphous ice: $T = 77$ K is considered) and glass transition temperature of glasses. TAS and 2S2G stand for $Te_2As_3Se_5$ and $Ga_2Ge_{20}Sb_{10}S_{65}$, respectively. E and R glasses are high strength industrial aluminosilicate glasses.

Fig. 1. Modules de Young à 293 K (à l'exception de la glace vitreuse : $T = 77$ K) et températures de transition vitreuse des verres. Les verres TAS et 2S2G ont pour formules respectives $Te_2As_3Se_5$ et $Ga_2Ge_{20}Sb_{10}S_{65}$. E et R désignent des verres aluminosilicatés industriels à haute résistance.

11 GPa for the densest ($\rho = 1.17$ g/cm^3) [46–48]. Chalcogenide glasses combine elements from the 16th column (VIB group) of Mendeleïev periodic table with metallic and/or semiconductor ones from the 13–15th columns. They consist of both strong covalent bonds between chain-forming chalcogen atoms (S, Se, Te) and atoms of higher coordination (As(3), Sb(3), Ge(4)) forming inter-chains bridges, and weak Van der Waals bonds between chains and/or layers. As a consequence of this weak intermolecular bonding, in spite of high covalent bond energies (200 to 400 kJ/mol), close to those of the Si–N and Si–C bonds, relatively weak glasses are obtained: $E < 25$ GPa ($T_g < 620$ K). As a matter of fact, heavy chalcogenide (or halide) elements which mostly appear in two-fold coordination lower the phonon vibration energy and thus enhance the infrared transparency. However weakly coordinated elements are detrimental to the network reticulation and therefore to the mechanical properties. When the bonding energy between a cation and an oxygen atom is greater than 500 kJ/mol, this cation is considered as a network former [49]. Such elements (P, Al, Ge, Zr, Si, B) gave their names to different oxide glass families with T_g ranging between 600 and 1300 K and Young's modulus between 30 and 100 GPa, the highest values being attributed to the aluminate glasses [11,21–23]. Although borate [50–52] and phosphate [53] glasses deteriorate in presence of water, they exhibit interesting chemical, thermal, optical or electronic properties. Germanate glasses [17] are transparent in the 2–6 μm infrared wavelength range and possess a good chemical durability.

1.2. The different scales concerned

In order to understand the elastic properties of known glasses or even better, to predict those of glasses which have not yet been synthesized, it is necessary to study the organization at the atomic scale. Elastic moduli do not solely depend on the interatomic bonding energy but also depend on the coordination, on the polymerization degree (reticulation), on the atomic packing density and on the molecular organization, including the possible formation of ring, chain or layer units. This calls for a multiscale approach. At first glance, the four relevant scales of concern are: (i) the atomic one, over 1.5 to 2.5 Å; (ii) the molecular one, from 2.5 to 4.5 Å; (iii) the 'network' one, within a few nanometers; and (iv) the continuum scale, over a hundred of nanometers. These scales are illustrated in Fig. 2. Scales (i) and (ii) are associated to the short range order which can be studied by nuclear magnetic resonance, Raman scattering spectroscopy, neutron scattering [20] or atomic force microscopy [54] for instance. At the network scale some kind of symmetry shows up beyond the atomic and molecular disorder with the formation of chains, as in pure selenium $(-Se-)_n$, layers as in the $Si_2Na_2O_3$ glass which consists of $SiO_{5/2}{}^{-}-Na^{+}$ units and eventually nanodomains making the glass a nanostructured material. Even though this latter scale is partly experimentally accessible by means of X-ray absorption spectroscopy (EXAFS) or by low frequency Raman scattering, it still remains poorly understood [55–57]. Scale (iv) is ruled by standard continuum mechanics equations and extends to the macroscopic scale of the useful functional part. Note, however, that the transition from the lower end of the continuum scale to the macro-scale still raises major technological difficulties for brittle materials.

2. Key parameters

2.1. Atomic scale

The elastic properties depend much on the chemico-physical properties of the interatomic bonds. Unfortunately, fundamental characteristics such as the interatomic distance (d), the directionality or the coordination (n) of every atom in its current situation in the glass are usually not accurately known. Under such circumstances, bonding energies [49, 57] and field strength [58] are mostly roughly estimated and can only give tendencies within given glass systems. Besides, based on a purely electrostatic interaction, the field strength approach suits quite well oxide glasses but becomes more and more questionable as the covalency of the interatomic bonding increases, such as in nitride and carbide systems. The situation is even more complex when weak Van der Waals type bonds co-exist with strong covalent bonds, as in chalco-halogenide glasses.

Another major parameter is the glass atomic packing density (C_g) defined as the ratio between the minimum theoretical volume occupied by the ions and the corresponding effective volume of glass:

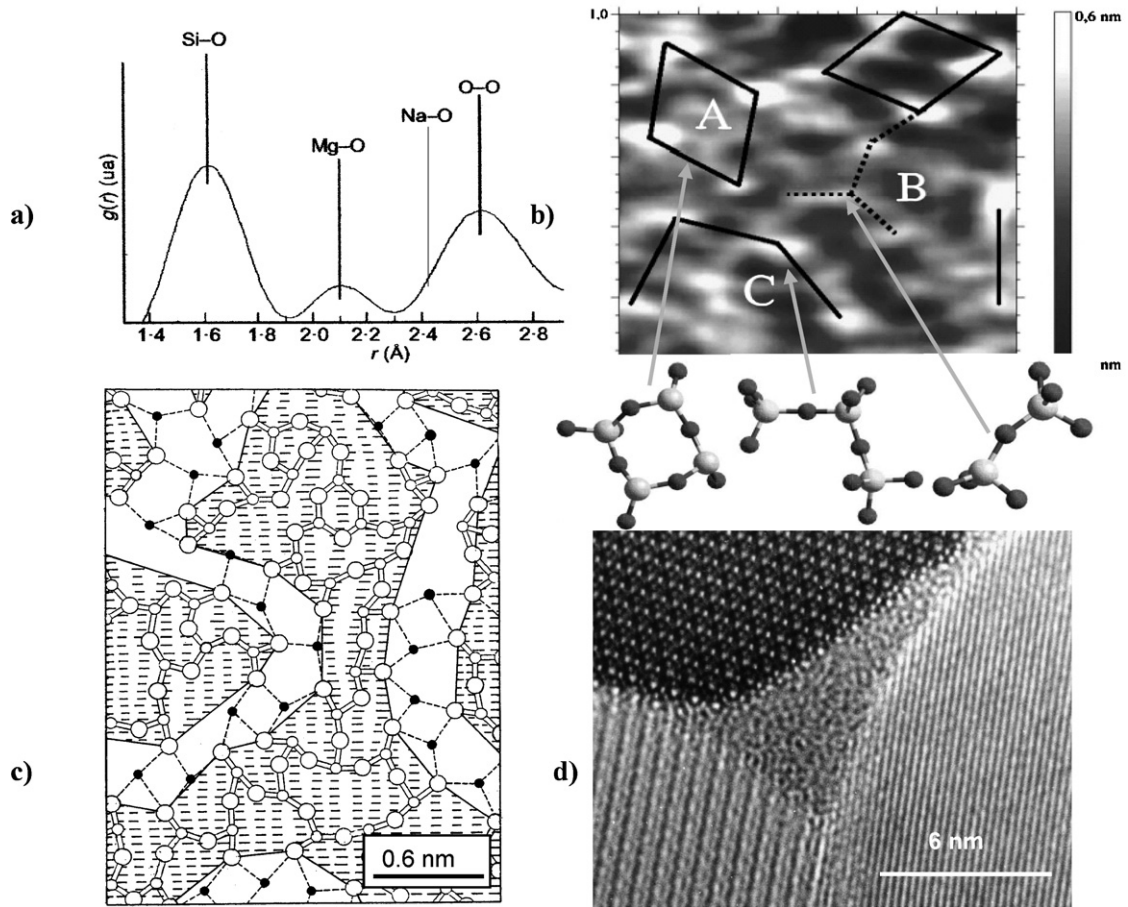$$C_g = \rho \sum f_i V_i / \left(\sum f_i M_i \right) \tag{1}$$

Fig. 2. The relevant scales: (a) The interatomic bond—correlation distribution function for a glass belonging to the SiO_2–Na_2O–MgO system (neutron diffusion, after Deriano et al. [20]); (b) The structural units (here the SiO_4 tetrahedron) and their possible combinations (atomic force microscopy)—a-SiO_2 case, after Poggemann et al. [54]; (c) The supramolecular scale—the modified random network proposed by Greaves [55] and supposing the existence of alkali-rich (solid circles) percolating channels; (d) The long range scale—glassy pocket at a triple grain junction in a Si_3N_4-based ceramics, after Rouxel et al. [56].

Fig. 2. Différentes échelles dont dépendent les propriétés mécaniques des verres : (a) La liaison interatomique—fonction de distribution de corré-lation pour un verre du système SiO_2–Na_2O–MgO (diffusion des neutrons), d'après Dériano et al. [20] ; (b) Les unités structurales (ici le tétraèdre SiO_4) et leurs combinaisons (microscopie à force atomique)—cas de la silice vitreuse, d'après Poggemann et al. [54] ; (c) L'échelle supramolé-culaire—le réseau aléatoire modifié proposé par Greaves [55] et faisant apparaître des canaux de percolation des cations modificateurs de réseau (cercles pleins) ; (d) Le désordre à longue distance—poche vitreuse au joint des grains dans une céramique de type nitrure de silicium, d'après Rouxel et al. [56].

with for the ith constituent with $A_x B_y$ chemical formula: $V_i = 4/3\pi N(x r_A^3 + y r_B^3)$, where ρ is the specific mass, N is Avogadro number, r_A and r_B are the ionic radii [57,59], f_i is the molar fraction and M_i is the molar mass.

For instance, C_g is about 0.52 for a standard window glass and 0.45 for a-SiO_2. An estimation of the packing density in metallic glasses was obtained by giving the atomic radius of each element its value in the corresponding pure metal. High pressure experiments ($P > 15$ GPa) and numerical simulations on disordered packings seem to indicate that maximum expected C_g values are about 0.65, whereas ordered systems with interstial species may reach C_g values higher than 0.74 (theoretical optimum for face-centered cubic simple body) [60,61]. Note, however, that relatively high values (>0.75) are obtained for multicomponent (mixtures of small and large atoms) metallic glasses, consistently with the remarkably high elastic moduli of these glasses.

Both interatomic energies (U_o) and atomic packing densities have to be taken into account to interpret elasticity data. For example, the substitution of Ca for Mg in a soda–lime–silica glass with 75 mol% SiO_2 and 15 mol% Na_2O does not lead to a stiffness increase as would be anticipated from the values of the bonding energies ($U_{oMg–O} >$

$U_{o\text{Ca–O}}$): both T_g and E decrease [20]. This is due to a significant decrease of C_g. The same explanation holds for the decrease of the stiffness observed in the same glass system when Mg is replaced by Si. Although $U_{o\text{Si–O}} > U_{o\text{Ca–O}} > U_{o\text{Mg(VI)–O}} > U_{o\text{Na–O}}$, C_g decreases as the Si content increases.

2.2. The 'molecular scale'

This scale is the one of the reticulation (polymerization) of the glass network with the occurrence of uni-, bi-, or tri-dimensional units. This reticulation greatly affects the elastic moduli. In the Ge–Se system, T_g and E increase with the Ge content whereas $U_{o\text{Ge–Ge}} < U_{o\text{Ge–Se}} < U_{o\text{Se–Se}}$. This trend stems from the change in the molecular architecture or in the medium range network topology. Four-fold coordinated Ge atoms increase the cross-linking degree and the network dimensionality. The glass network evolves from a mixture of chain-like units to a mixture of layer-like units and further to a tri-dimensional organization. In regard to pure Se glass consisting of chains and rings, with $T_g = 313$ K and $E = 10.2$ GPa, a $Ge_{0.4}Se_{0.6}$ glass exhibits much better properties: $T_g = 613$ K and $E = 22.4$ GPa [43]. In this case, the mean coordination number ($\langle n \rangle$) [62,63] is a useful tool to correlate the physical properties to the structural changes. For example, for a Ge_xSe_{1-x} ($x \leqslant 1$) glass, this number writes: $\langle n \rangle = 2(x + 1)$. As far as $\langle n \rangle$ is less than 2.1, the volume fraction of Ge-containing chains is negligible so that deformation essentially proceeds through the alignment of the chains with the main loading axis in tension or in transverse planes in compression. In this case properties are mainly governed by the weak Van der Waals forces. As n increases, covalent bonds come into play. A so-called 'rigid percolation threshold' is reached for $\langle n \rangle = 2.4$ ($GeSe_4$ composition) corresponding to a complete reticulation of the glass network consisting of Se and Ge layer units, two neighbouring Ge atoms being separated by two Se atoms. At $\langle n \rangle = 2.67$ ($GeSe_2$ stoichiometry), Ge–Ge starts to form and a tri-dimensional network builds up. A significant increase of E and T_g follows, but the glass becomes more brittle at the same time [43]. A comparable situation exists in borate glasses. In this latter case, the stiffness predicted from the interconnected layers of BO_3 triangles is greatly overestimated due to the presence of weak inter-layers bonds. For oxide glasses, the number of bridging oxygen atoms per tetrahedron (SiO_4 or AlO_4 for instance), n_{OP}, provides a measurement of the network reticulation degree and flexibility. Let us consider the concentrations in oxygen [O] and in network forming
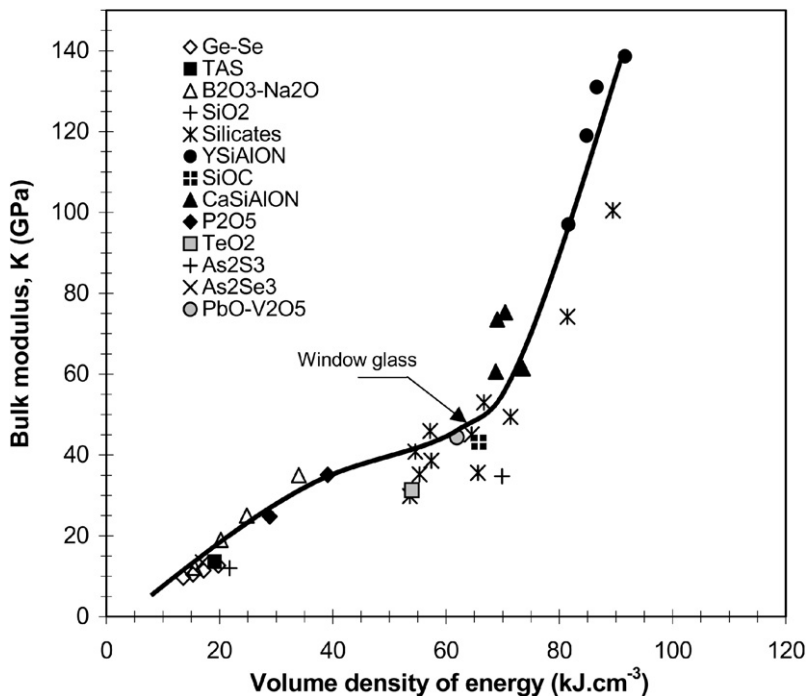

Fig. 3. Experimental bulk modulus as a function of the calculated volume density of energy.

Fig. 3. Module de compressibilité expérimental en fonction de la densité volumique d'énergie calculée.

elements, [Si*], where, for a glass containing Si, Al and Zr, [Si*] stands for [Si] + [Al] + [Zr], the estimation of n_{OP} is straightforward. For a $(SiO_2)_w(Al_2O_3)_x(CaO)_y(Na_2O)_z$ glass, assuming all Al atoms are 4-fold coordinated, this number is given by: $n_{OP} = 4 - 2(y + z - x)/(w + 2x)$. An extension to the cases of oxycarbide and oxynitride glasses is obtained by replacing [O] by an equivalent anionic concentration [O*], with [O*] = [O] + 3/2[N] and [O*] = [O] + 2[C] for N and C containing glasses respectively. Nuclear magnetic resonance measurements lead mostly to experimental n_{OP} values very close to the theoretical ones. Oxynitride and oxycarbide glasses provide a good illustration of the impact of the glass network cross-linking degree on the elastic moduli. Oxynitride glasses are much stiffer and refractory ($T_g > 1173$ K) than their parent oxide glasses (same cationic species). Oxycarbide glasses are even more refractory (Fig. 1). However, the values for the bonding energies do not corroborate this tendency: U_{oSi-C} (447 kJ/mol) $\approx U_{oSi-N}$ (437 kJ/mol) $< U_{oSi-O}$ (800 kJ/mol). Photoelectron spectroscopy (XPS) measurement on Si confirmed the presence of lower energies (Fermi levels) in oxycarbide environments than in oxide (SiO$_2$) ones [64]. Hence, similar to what governs the rigidity of steel frames, the source for the excellent stiffness of oxynitride and oxycarbide glasses lies in the 3D bonding architecture rather than in the bond strength itself. Note however that this reasoning may be greatly complicated in some cases due to possible phase separations (chain-forming chalcogen atoms tend to stay together in chalcogenide glasses) or clustering (rings formed upon 5, 6, 7 or 8 SiO$_4$ tetrahedra in a-SiO$_2$, Se$_8$ rings in Se-based glasses).

2.3. Mesoscopic or 'supramolecular' scale

A glass is a solid with a small length of coherency, with respect to optical wavelengths for instance. However, in most glasses, including metallic ones, few nanometer large nano-domains seem to exist. Glasses would hence possess some organization at a mesoscopic scale. The size of the domains, which are likely to be amorphous, is typically less than 10 nm and can be estimated from the frequency of the 'Boson' peak observed in the 3–50 cm^{-1} Raman frequency range. The estimated correlation lengths, in good agreement with first diffraction peak measurements, are much larger than the characteristic distances of the short range order. In the light of these investigations, glass appears as a nano-composite material consisting of islands immerged in a more easily deformable softer phase, especially at high temperature.

2.4. Scale change: from the bond to the continuum

Elastic moduli depend chiefly on the interatomic bonding energy and on the atomic packing density. Both ingredients are included in the expression for the bulk elastic modulus (K) which derives from the form of the interatomic potential. In the simplistic case of a Lennard-Jones type potential it comes (1st Grüneisen rule [65]):

$$K = V_o \frac{\partial^2 U}{\partial V^2}\bigg|_{V_o} = \frac{mn}{9V_o}U_o \tag{2}$$

where U_o is the atomic bonding energy, V_o is the atomic volume at equilibrium and m and n are the exponents of the power law describing the attractive and the repulsive terms, respectively.

It appears that K is proportional to a volume density of energy. In the case of glasses neither the atomic volumes nor the bonding energy are accurately known. Furthermore, m and n depend on the chemical nature of the bonds and are likely to fluctuate with the composition. Nevertheless, the former expression gave birth to several theoretical models aimed at providing ab initio values for the elastic moduli [16,66]. The most widely used model is that proposed by Makishima et al. [16] which expresses E as a function of the volume density of energy and C_g (Eq. (1)). The energy density is calculated from the dissociation (or atomization) energies of the different oxides introduced in the starting powder mixture. Although the theoretical prediction of E, as well as the tendencies through series of silicate glasses are quite satisfactory, the elastic moduli of phosphate and borate glasses are greatly overestimated. In phosphates, this is due to the presence of double P=O bonds which do not contribute to the network stiffness (the oxygen atom is not bridging), so that the corresponding energy should be subtracted from the dissociation energy of the P$_2$O$_5$ compound. In borates, the overestimation originates from the weak bonds between the planar BO$_3$ triangle (to be compared to the B$_2$O$_3$ crystal built on BO$_4$ units). On the other hand, E is underestimated in the case of germanate, aluminate and high modulus glasses, in general. Let us examine the dependence of K on the atomization (dissociation) enthalpy, which is

a measurement of the mean atomic network energy. For a multi-constituent glass this enthalpy can be estimated from the properties of the constituents according to:

$$\left\langle \frac{U_o}{V_o} \right\rangle = \sum f_i \Delta H_{ai} \Big/ \left(\sum f_i M_i / \rho_i \right) \tag{3}$$

where ΔH_{ai} is the atomization enthalpy per mole of the ith constituent, ρ_i is the specific mass, f_i and M_i are the molar fraction and the molar mass, respectively, with for the ith constituent written $A_x B_y$, according to an ordinary Born–Haber cycle:

$$\Delta H_{ai} = x \Delta H_f^o(A, g) + y \Delta H_f^o(B, g) - \Delta H_f^o(A_x B_y) \tag{4}$$

The standard formation enthalpy of a cation is equal to its sublimation enthalpy whereas for an anion gaseous in its standard state, the molar dissociation energy of the gas molecules must be considered. The denominator in the right-hand side in Eq. (3) represents the whole volume occupied by the atoms of an 'equivalent' mole of glass provided the volume occupied by each atom is the same as in the crystal of the raw material introduced during the synthesis. The presence of free volume in the glass and therefore of an atomic packing density lower than the one of a crystallized solid with same composition is thus not taken into account in this ab initio approach. Values for the dissociation energy in phosphate and borate glasses were corrected on the basis of structural information following Makishima et al. [16]. In the case of $SiO_{1.6}C_{0.8}$, the dissociation energy was estimated assuming a synthesis from SiC (12.5%), SiO_2 (0.5%) and C (0.375%) whereas a polymer route leaving some free carbon in the material was used. For the residual carbon an intermediate density between the ones of graphite and diamond was chosen. In the case of chalcogenide glasses little information was available regarding the thermodynamics of the studied compositional systems. Therefore the atomization enthalpies were estimated following a procedure proposed by Shkol'nikov [67] and based on the atomic bonding energies and coordinations:

$$\Delta H_{ai} = N \langle U_o \rangle \langle n_c \rangle \tag{5}$$

where $\langle U_o \rangle$ and $\langle n_c \rangle$ are the mean covalent bonding energy and the average number of covalent bonds per atom, respectively. This number $\langle n_c \rangle$ turns out to be half the mean coordination number: $\langle n_c \rangle = \langle n \rangle / 2$. For instance, for $GeSe_4$ glass: $\langle U_o \rangle = 1/3(U_o(Se–Se) + 2U_o(Ge–Se))$ and $\langle n_c \rangle = 6/5$.

3. Discussion

3.1. Atomic bond scale and packing density

One way to improve the volume density of energy of a glass is through cationic substitutions, looking for the optimum compromise between glass formers, possessing high bonding energies but leading to relatively low packing densities, and modifying cations, favouring a high value for C_g but introducing relatively weak bonds. Among electropositive elements, i.e. which tend to form cations, the less electropositive ones favour glass formation and hence do not contribute to the filling of interstitial sites and thus may be detrimental to the elastic moduli. Finally, best results are obtained with intermediate elements such as Hf, Be, Zr, Ti, Li and Th for which (except for Li) the electronegativity (Pauling's scale) is between 1.25 and 1.75 [21]. So far, highest elastic moduli values ($E = 145$ GPa) were obtained with Mg-aluminates containing more than 25 mol% BeO (eminently toxic oxide), for the synthesis of reinforcement fibers. Aluminosilicate glasses are used when a high strength is desired: E- (with boron), R- (without boron) and S- (with Mg) glasses (Fig. 1) with strength (pristine fiber) up to 3.2 to 4.2 GPa are available. High elastic moduli are also obtained with the addition of rare earth (RE) oxides ($E = 110$–135 GPa), best results being obtained with the smallest RE-cations (Sc, Lu, Yb, Y) [34].

A more efficient way consists in replacing some oxygen atoms by anions with higher valency, such as trivalent nitrogen or even tetravalent carbon ions. The network reticulation degree is increased and a rigidity improvement follows. Oxynitride glasses are a good example of this approach. To the best of the author's knowledge, the highest Young's modulus reported so far for an inorganic non-metallic glass is $E = 186$ GPa for $Y_{0.15}Si_{0.15}Al_{0.1}O_{0.35}N_{0.15}$ [68]. Nevertheless, the substitution of oxygen for carbon in a-SiO_2 does not bring the expected enhancement. The reason lies in the low packing density in oxycarbide glasses. The atomic network compactness and the bonding energy are the parameters governing the elastic moduli. Accordingly, the bulk elastic modulus correlates with the
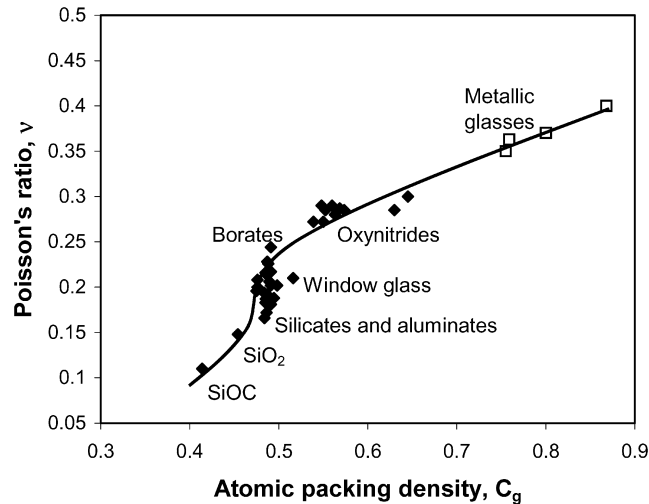
Fig. 4. Poisson's ratio and atomic network packing density.

Fig. 4. Coefficient de Poisson et densité d'empilement atomique du réseau vitreux.

volume density of energy (Fig. 3) with a linear dependence, $K = U_o/V_o$, as long as $U_o/V_o < 50 \, \mathrm{kJ/cm^3}$, which gives $m = 9$ and $n = 1$ in Eq. (2). Instead, T_g seems to depend mostly on the mean bonding energy. As a matter of fact, the low density a-SiO$_2$ and oxycarbide glasses are very refractory but exhibit elastic moduli close to those of metallic glasses, far less refractory but much more compact (Fig. 1).

3.2. The molecular scale

The molecular scale governs the glass network compactness and dimensionality (i.e., the occurrence of a medium-range order showing up through the formation of chain (D1) or layer (D2) units or of a tri-dimensional reticulation (D3)). Poisson's ratio plays a very interesting role here. It seems indeed that the knowledge of ν suffices to evaluate C_g (Fig. 4) and to estimate the network dimensionality (Fig. 5). Although C_g values cannot be accurately measured, mainly because of the lack of actual atomic radius data (provided it has a meaning), the relatively wide spectrum of glasses investigated in this review, with different types of atomic bonds, shows a clear trend: C_g increases monotonically with ν, from about 0.41 for an SiOC glass ($\nu = 0.11$) to about 0.87 for a PdCuNi glass ($\nu = 0.4$). This suggests that densification of glasses under high pressure such as that existing beneath a Vickers indenter is favoured by low Poisson's ratio. On the contrary, shear plasticity is expected in glasses with high ν values, consistent with recent observations [69]. Moreover, ν reflects the glass dimensionality. The network reticulation degree and dimensionality increase when ν decreases. Although data spread over a relatively large zone, it is noteworthy that, through a given glass series, ν depends linearly on $\langle n \rangle$ or $\langle n_{\mathrm{OP}} \rangle$. A glass with $\nu < 0.17$ is predominantly 3D, whereas for $\nu > 0.27$ chain units prevail. Interestingly, a strong chemical disorder, corresponding to little ordering at both medium and short ranges, corresponds to small $\langle n \rangle$ or $\langle n_{\mathrm{OP}} \rangle$ values, eventually less than unity, and to ν tending towards 0.5, which is precisely the value for liquids which deform with little (no) volume change.

3.3. Mesoscopic scale

The temperature dependence of the elastic moduli of composite materials is strongly governed by the softening of the less refractory phase (grain-boundary glassy phase in liquid-phase sintered ceramics such as in Fig. 2(d)). In analogy, the sensitivity of the elastic moduli of glasses to temperature is expected to bring an interesting light on the possible existence of a supra-molecular or mesoscopic architecture. Ultrasonic [30,37,70–72] or mechanical spectroscopy [73,74] investigations of the temperature dependence of Young's modulus in different glass systems reveal a slow decrease of E with T up to T_g followed by a faster decrease in the super-cooled liquid range ($T > T_g$) (Fig. 1). There seems to be two kinds of behavior. For relatively stiff glasses with $E > 10 \, \mathrm{GPa}$ and for $T_g \leqslant T \leqslant 1.1 T_g$, $E = E(T_g) T_g / T$. Less rigid glasses exhibit a faster decrease of E with T. Therefore, it seems that the temperature
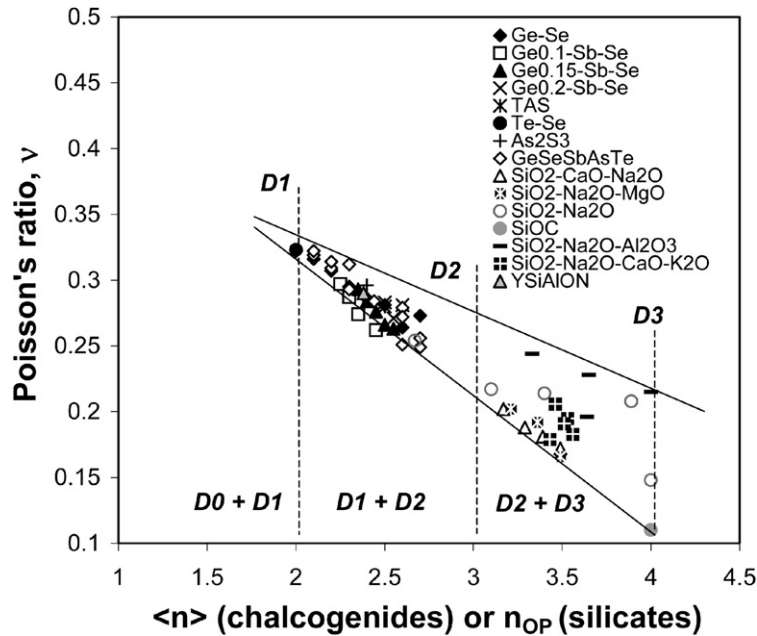
Fig. 5. Relationship between Poisson's ratio and the glass network dimensionality. D0 reflects a high chemical disorder with a weak bond directionality and a low cross-linking degree. D1, D2 and D3 indicate the formation of chain, layer and tri-dimensional units, respectively.

Fig. 5. Relation entre le coefficient de Poisson et la dimensionnalité du réseau vitreux. D0 indique un grand désordre chimique avec une faible directionnalité des liaisons et une faible réticulation du réseau vitreux. D1 correspond à la formation de chaînes. D2 indique la formation de feuillets et D3 d'une organisation tri-dimensionnelle.

dependence of the Young's modulus reflects the degree of 'fragility' (as defined by Angell [75]) of the glass. It is suggested that the fast softening of a glass above T_g reveals the existence of nano-domains (island organization) embedded in a softer phase. This hypothesis is supported by activation volume (V_a) data as determined from creep experiments: $V_a^{1/3} \approx 0.6$ nm for Zr-based metallic glasses [76] and 2 nm for SiYAlON glasses [2]. These values are comparable to those obtained from a local probing [77] and are corroborated by recent structural studies in metallic glasses [78]. Additional structural and mechanical investigations are clearly needed to get more insight in this area.

4. Summary and perspectives

Elastic moduli are relatively easily measurable macroscopic parameters. It is shown in this study that they can be used to probe the glass network architecture both at the nano-, micro- and meso-scopic scales. Comparative investigations conducted on series of glasses from different glass systems, including metallic, ionic and covalent bonding, reveal the following tendencies:

(1) There is a direct relationship between the bulk modulus and the volume density of energy (no such correlation exists between elastic moduli and T_g).
(2) Poisson's ratio (ν) correlates with the atomic packing density (C_g) and with the glass network dimensionality. The atomic packing density C_g increases with ν. Poisson's ratio ν ranges from ~0.1 for a SiOC glass characterized by a large fraction of free volume, to ~0.4 for Pd- and Zr-based bulk metallic glasses. The network dimensionality (chains, layers, etc.) increases monotonically with the mean coordination number or with the fraction of bridging oxygen atoms per tetrahedron, but changes inversely with ν. Hence, for chalcogenide glasses, the network of which resembling the one of chain-polymers, $\nu > 0.25$, whereas in the case of tri-dimensional organisation, such as in SiO_2-rich glasses, $\nu < 0.2$.
(3) The temperature dependence of the Young's modulus allows for an estimation of the glass fragility and opens interesting perspectives towards a mesoscopic approach of the glass response to mechanical testing.

Acknowledgements

References

[1] J.C. Thompson, K.E. Bailey, J. Non-Cryst. Sol. 27 (1978) 161–172.
[2] T. Rouxel, M. Huger, J.L. Besson, J. Mat. Sci. 27 (1992) 279–284.
[3] M. Ohtsuki, R. Tamura, S. Yoda, T. Ohmura, Appl. Phys. Lett. 84 (2004) 4911.
[4] A. Inoue, Mat. Sci. Trans., JIM 36 (7) (1995) 866–875.
[5] W.L. Johnson, Mat. Sci. Forum 225–227 (1996) 35–50.
[6] A. Inoue, Bulk Amorphous Alloys, Practical Characteristics and Applications, Mat. Sci. Fund., vol. 6, Trans. Tech. Pub. Inc., Switzerland, 1999.
[7] J. Philibert, A. Vignes, Y. Bréchet, P. Combrade, Métallurgie: du minerai au matériau, Masson, Paris, 1998.
[8] W.H. Wang, J. Non-Cryst. Sol. 351 (2005) 1481–1485.
[9] S. Tanabe, K. Hirao, N. Soga, J. Am. Ceram. Soc. 75 (3) (1992) 503–506.
[10] A. Makishima, Y. Tamura, T. Sakaino, J. Am. Ceram. Soc. 61 (5–6) (1978) 247–249.
[11] X. Zou, H. Toratami, J. Non-Cryst. Sol. 290 (2001) 180–188.
[12] S. Inaba, S. Fujino, K. Morinaga, J. Am. Ceram. Soc. 82 (12) (1999) 3501–3507.
[13] L.G. Hwa, T.H. Lee, S.P. Szu, Mat. Res. Bull. 39 (2004) 33–40.
[14] C.J. Phillips, Glass Tech. 5 (6) (1964) 216–223.
[15] M.L. Williams, G.E. Scott, Glass Tech. 11 (3) (1970) 76–79.
[16] A. Makishima, J.D. Mackenzie, J. Non-Cryst. Sol. 12 (1973) 35–45;
     A. Makishima, J.D. Mackenzie, J. Non-Cryst. Sol. 17 (1975) 147–157.
[17] B. Bridge, N.D. Patel, D.N. Waters, Phys. Stat. Sol. (a) 77 (1983) 655–668.
[18] N. Soga, J. Non-Cryst. Sol. 73 (1985) 305–313.
[19] B. Bridge, A.A. Higazy, Phys. Chem. Glasses 27 (1) (1986) 1–14.
[20] S. Deriano, T. Rouxel, M. LeFloch, B. Beneu, Phys. Chem. Glasses 45 (1) (2004) 37–44.
[21] K.L. Loewenstein, Phys. Chem. Glasses 2 (3) (1961) 69–82.
[22] V.Ya. Livshits, D.G. Tennison, S.B. Gukasyan, A.K. Kostanyan, Soviet J. Glass Phys. Chem. 8 (1982) 463–468.
[23] W. Capps, D.H. Blackburn, A.A. Edwards, M. Black, Nat. Bur. Stand. Reports, 3978, 4176, 4318, 4417, 4699, 4850 and 5188, 1955–1957.
[24] R.E. Loehman, J. Non-Cryst. Sol. 56 (1983) 123–134.
[25] S. Hampshire, R.A.L. Drew, K.H. Jack, J. Am. Ceram. Soc. 3 (1984) C46.
[26] J. Rocherullé, C. Ecolivet, M. Poulain, P. Verdier, Y. Laurent, J. Non-Cryst. Sol. 108 (1989) 187–193.
[27] A. Sekkat, S. Etienne, C. Maï, J. Perez, C. Garnier, P. Verdier, Y. Laurent, J. Phys. IV, Coll. C2, Supp. J. Phys. III, vol. 2, 1992, pp. C2-253–256.
[28] C. Ecolivet, P. Verdier, Mat. Res. Bull. 19 (1984) 227–231.
[29] S. Hampshire, E. Nestor, R. Flynn, J.L. Besson, T. Rouxel, H. Lemercier, P. Goursat, M. Sebai, D.P. Thompson, K. Liddell, J. Europ. Ceram. Soc. 14 (1994) 261–273.
[30] H. Lemercier, T. Rouxel, D. Fargeot, J.L. Besson, B. Piriou, J. Non-Cryst. Sol. 201 (1996) 128–145.
[31] E.Y. Sun, P.F. Becher, S.L. Hwang, S.B. Waters, G.M. Pharr, T.Y. Tsui, J. Non-Cryst. Sol. 208 (1996) 162–169.
[32] R. Daucé, P. Verdier, Y. Laurent, J.A. Odriozola, Ann. Chim. Sci. Mat. 28 (2003) 79–86.
[33] P.F. Becher, M.J. Lance, M.K. Ferber, M.J. Hoffman, R.L. Satet, J. Non-Cryst. Sol. 333 (2004) 124–128.
[34] F. Lofaj, S. Dériano, M. LeFloch, T. Rouxel, M.J. Hoffmann, J. Non-Cryst. Sol. 344 (2004) 8–16.
[35] J. Homeny, G.G. Nelson, S.H. Risbud, J. Am. Ceram. Soc. 71 (5) (1988) 386–390.
[36] G.M. Renlund, S. Prochazka, R.H. Doremus, J. Mat. Res. 6 (12) (1991) 2723–2734.
[37] G.D. Soraru, E. Dallapicola, G. D'Andrea, J. Am. Ceram. Soc. 79 (8) (1996) 2074–2080.
[38] T. Rouxel, G. Massouras, G.-D. Soraru, J. Sol–Gel Sci. Technol. 14 (1999) 87–94.
[39] T. Rouxel, G.D. Soraru, J. Vicens, J. Am. Ceram. Soc. 84 (5) (2001) 1052–1058.
[40] C. Moysan, R. Riedel, R. Harshe, T. Rouxel, F. Augereau, J. Eur. Ceram. Soc., in press.
[41] S. Mahadevan, A. Giridhar, A.K. Singh, J. Non-Cryst. Sol. 57 (1983) 423–430.
[42] A.N. Sreeram, A.K. Varshneya, D.R. Swiler, J. Non-Cryst. Sol. 128 (1991) 294–309.
[43] V.Q. Nguyen, J.S. Sanghera, I.D. Aggarwal, I.K. Lloyd, J. Am. Ceram. Soc. 83 (4) (2000) 855–859.
[44] J.P. Guin, T. Rouxel, J.C. Sangleboeuf, I. Melscoët, J. Lucas, J. Am. Ceram. Soc. 85 (6) (2002) 1545–1552.
[45] A. Delben, Y. Messaddeq, M.D. Caridade, M.E. Aegerter, J. Non-Cryst. Sol. 161 (1993) 165–168.
[46] J.C. Thompson, K.E. Bayley, J. Non-Cryst. Sol. 27 (1978) 161–172.

[47] J. Hessinger, B.E. White, R.O. Pohl, Planet. Space Sci. 44 (9) (1996) 937–944.
[48] M.M. Koza, B. Geil, H. Schober, F. Natali, Phys. Chem. Chem. Phys. 7 (2005) 1423–1431.
[49] http://en.wikipedia.org/wiki/Amorphous_ice;
      See also: http://www.lsbu.ac.uk/water/index.html.
[50] K.H. Sun, J. Am. Ceram. Soc. 30 (1947) 277–281.
[51] J.F. Ducel, J.J. Videau, Mat. Lett. 18 (1993) 69–72.
[52] S. Singh, A.P. Singh, S.S. Bhatti, J. Mat. Sci. 24 (1989) 1539–1542.
[53] I.Z. Hager, J. Mat. Sci. 37 (2002) 1309–1313.
[54] K.H. Chang, T.H. Lee, L.G. Hwa, Chin. J. Phys. 41 (4) (2003) 414–421;
      See also: http://www.ceramics.nist.gov/srd/summary/glspho.htm.
[55] J.F. Poggemann, A. Goss, G. Heide, E. Rädlein, G.H. Frischat, J. Non-Cryst. Sol. 281 (2001) 221–226.
[56] G.N. Greaves, J. Non-Cryst. Sol. 71 (1985) 203–217.
[57] A.P. Sokolov, A. Kisliuk, M. Soltwisch, D. Quitman, Phys. Rev. Lett. 69 (10) (1992) 1540–1543.
[58] E. Duval, A. Boukenter, T. Achibat, J. Phys. Cond. Matter 2 (1990) 10227–10234.
[59] T. Rouxel, F. Wakai, Acta Met. Mat. 41 (11) (1993) 3203–3213.
[60] D.R. Lide (Ed.), Handbook of Chemistry and Physics, 86th ed., Taylor & Francis, 2005–2006.
[61] A. Dietzel, Glastech. Ber. 22 (1948–1949) 212.
[62] R.D. Shannon, Acta Cryst. A 32 (5) (1976) 751–767.
[63] T. Aste, M. Saadatfar, A. Sakellariou, T.J. Senden, Physica A 339 (2004) 16–23.
[64] T.M. Truskett, S. Torquato, P.G. Debenedetti, Phys. Rev. E 62 (1) (2000) 993–1001.
[65] J.C. Phillips, J. Non-Cryst. Sol. 34 (1979) 153–181.
[66] K. Tanaka, Phys. Rev. B 39 (1989) 1270–1279.
[67] G.D. Soraru, G. D'Andrea, A. Glisenti, Mat. Lett. 27 (1996) 1–5.
[68] D.R. Messier, A. Broz, J. Am. Ceram. Soc. 65 (8) (1982) C-123.
[69] C. Zwikker, Grüneisen 1st rule, in: Physical Properties of Solid Materials, Wiley Interscience, New York, 1954, p. 90.
[70] M.L. Cohen, Phys. Rev. B 32 (12) (1985) 7988–7991.
[71] E.V. Shkol'nikov, Soviet J. Glass Phys. Chem. 11 (1985) 40–44.
[72] S. Yoshida, J.C. Sangleboeuf, T. Rouxel, J. Mat. Res. 20 (2005) 3404–3412.
[73] T. Rouxel, J.C. Sangleboeuf, J. Non-Cryst. Sol. 271 (2000) 224–235.
[74] T. Rouxel, J.C. Sangleboeuf, M. Huger, C. Gault, J.-L. Besson, S. Testu, Acta Mat. 50 (2002) 1669–1682.
[75] Keryvin, M.-L. Vaillant, T. Rouxel, M. Huger, T. Gloriant, Y. Kawamura, Intermetallics 10 (2002) 1289–1296.
[76] E. Le Bourhis, P. Gadaud, J.-P. Guin, N. Tournerie, X.-H. Zhang, J. Lucas, T. Rouxel, Scripta Mat. 45 (2001) 317–323.
[77] P. Gadaud, S. Pautrot, J. Non-Cryst. Sol. 316 (2003) 146–152.
[78] C.A. Angell, J. Phys. Chem. Sol. 49 (8) (1988) 863–871.